Creation of X-Ray Transparency of Matter by Stimulated Elastic Forward Scattering

J. Stöhr[1,*] and A. Scherz[2,†]

[1]*SLAC National Accelerator Laboratory, 2575 Sand Hill Road, Menlo Park, California 94025, USA*
[2]*European XFEL GmbH, Albert-Einstein-Ring 19, 22761 Hamburg, Germany*

X-ray absorption by matter has long been described by the famous Beer-Lambert law. Here, we show how this fundamental law needs to be modified for high-intensity coherent x-ray pulses, now available at x-ray free electron lasers, due to the onset of stimulated elastic forward scattering. We present an analytical expression for the modified polarization-dependent Beer-Lambert law for the case of resonant core-to-valence electronic transitions and incident transform limited x-ray pulses. Upon transmission through a solid, the resonant absorption and dichroic contrasts are found to vanish with increasing x-ray intensity, with the stimulation threshold lowered by orders of magnitude through a resonant superradiantlike effect. Our results have broad implications for the study of matter with x-ray lasers.

Nonlinear interactions of intense electromagnetic radiation with matter have long been utilized in the microwave and optical regions to control nuclear and valence electronic transitions and have enabled breakthroughs in many fields of science, such as medical imaging, telecommunication, or the creation and manipulation of novel states of matter. The natural extension of these techniques into the x-ray region had to await the availability of sufficiently bright x-ray sources in the form of x-ray free electron lasers. Over the last few years, several experiments performed with rather uncontrolled x-ray pulses of high intensity, produced through the self-amplification of spontaneous emission (SASE) process [1], have revealed the presence of electronic stimulation [2] or multiple ionization [3] effects at extreme intensities ($\sim$10–1000 J/cm^2/fs).

Here, we discuss how x-ray transmission through matter can be modified in a controlled way by stimulated scattering effects induced by transform limited x-ray pulses now available through self-seeding [4]. The optical analogue of the x-ray effects discussed here is "self-induced transparency," first observed and theoretically treated by McCall and Hahn [5].

In contrast to stimulated inelastic scattering [2,6,7], which requires pulses with a broad bandwidth that covers the difference between excitation and deexcitation energies or multicolor pulses with separate "pump" and "dump" functions, we consider, here, the conceptually simpler case of elastic stimulation which exists within the energy bandwidth of the incident beam itself. In this case, stimulated x-ray scattering modifies the fundamental Beer-Lambert law because of the direct link of x-ray absorption and resonant elastic scattering through the optical theorem. For typical sample thicknesses of 1–2 x-ray absorption lengths, amplified spontaneous (inelastic) emission, is negligible because of the short gain length [8].

Of particular importance and interest are experiments that utilize resonant electronic core-to-valence transitions, since they exhibit large cross sections, provide elemental and chemical bonding specificity, and, through their polarization dependence, enable the determination of bond orientation [9] and the dichroic separation of charge and spin based phenomena [10]. Resonant x rays are widely utilized not only in absorption measurements, but also in x-ray microscopy [11], coherent x-ray imaging [12], and inelastic x-ray scattering [13]. Since resonant x-ray excitations occur within the atomic volume, the associated stimulated effects can mostly be described within an atom-based framework. For different forms of matter, the resonant x-ray response differs only through the atom-projected valence states, in contrast to the optical response. This makes the presented theory widely applicable.

We derive the modified Beer-Lambert law by utilizing the time-dependent density matrix approach where the evolution of the resonant core-valence two-level system is governed by the optical Bloch equations [14]. An analytical solution is obtained for the case of incident transform limited x-ray pulses whose coherence time is much longer than the core hole lifetime. We apply our theory to the important case of 3d transition metal samples whose polarization dependent transmission exhibits both a charge and spin response, the latter through the x-ray magnetic circular dichroism (XMCD) effect. We find that, for the prominent Co L_3 absorption resonance at 778 eV (wavelength of 1.6 nm), stimulated decays begin to rob intensity from the dominant spontaneous Auger channel at an incident intensity of $\sim$1–10 mJ/cm^2/fs, with the onset lowered by resonant coherent (super-radiant) enhancement by more than 2 orders of magnitude. At higher intensities, the sample becomes increasingly transparent with the spin-based XMCD contrast disappearing sooner than the charge-based absorption contrast.

We follow the formalism of Ref. [10] and, denoting the x-ray polarization by the labels $q = 0$ for linear, $q = +$ for right, and $q = -$ for left circular polarization, describe the polarization dependent x-ray response of a magnetic sample in terms of the atomic scattering length in the soft-x-ray approximation as $f^q(\vec{Q} = 0) = r_0 Z + f'^q - if''^q$, where r_0 is the Thomson scattering length and Z the atomic number. The spontaneously transmitted intensity through a sample of atomic number density ρ_a and thickness d is given by the Beer-Lambert law

$$I^q_{\text{trans}} = I^q_0 e^{-2\lambda f''^q \rho_a d}, \qquad (1)$$

where I^q_{trans} and I^q_0 are the polarization dependent transmitted and incident intensities and $\sigma^q_{\text{abs}} = 2\lambda f''^q$ is the x-ray absorption cross section. Our x-ray scattering length formulation is related to the optical constants and the electric susceptibility through the complex refractive index $\tilde{n}^q = 1 - \delta^q + i\beta^q \simeq 1 + \frac{1}{2}(\chi'^q + i\chi''^q)$, where $\delta^q = \rho_a \lambda^2 (r_0 Z + f'^q)/2\pi$ and $\beta^q = \rho_a \lambda^2 f''^q/2\pi$.

The resonant polarization dependent x-ray absorption cross section $\sigma^q_{\text{abs}} = 2\lambda f''^q$ and the differential atomic elastic scattering cross section $d\sigma^q_{\text{scat}}/d\Omega = (f'^q)^2 + (f''^q)^2$ have a Lorentzian line shape and are linked by the optical theorem which may be written as

$$f''^q = \frac{\Gamma}{\Gamma^q_x} \frac{2\pi}{\lambda} [(f'^q)^2 + (f''^q)^2]$$
$$= \frac{\Gamma^q_x}{\Gamma} \frac{\lambda}{2\pi} \frac{(\Gamma/2)^2}{(\hbar\omega - \mathcal{E}_0)^2 + (\Gamma/2)^2}. \qquad (2)$$

Here, $\mathcal{E}_0$ is the resonant photon energy, $\Gamma = \Gamma^q_x + \Gamma_A$ is the total spontaneous decay width, which, in the soft x-ray region, is dominated by the Auger width $\Gamma \simeq \Gamma_A$ [15]. The polarization dependent radiative transition widths Γ^q_x consist of a radial and angular part and can be calculated by *ab initio* methods. We have derived their values for Fe, Co, and Ni metal from experimental data, and they are listed in Table I.

The polarization dependent Lorentzian x-ray absorption cross sections $\sigma^q_{\text{abs}} = 2\lambda f''^q$ calculated with Eq. (2) and the parameters for Co in Table I are shown as blue curves in Fig. 1(a). They were derived from fits of the experimental resonant cross sections by Voigt profiles (red curves) shown
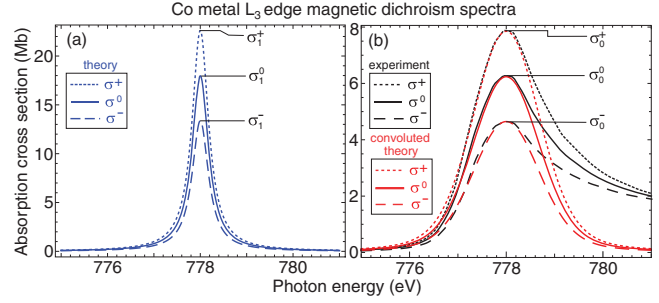

FIG. 1 (color). (a) Polarization and photon energy dependent L_3 absorption cross sections $\sigma^q_{\text{abs}} = 2\lambda f''^q$ for Co metal, calculated by use of Eq. (2) and the parameters Γ and Γ^q_x in Table I. (b) Comparison of the experimental dichroic cross sections (black lines) and the theoretical cross sections in (a) convoluted with a Gaussian of 1.4 eV FWHM. Note that the corresponding blue and red curves have the same areas, but their peak values differ by a factor of $\sigma^q_1/\sigma^q_0 = 2.9$.

in Fig. 1(b), consisting of a convolution of the natural Lorentzian line shapes in 1(a) with a Gaussian of 1.4 eV FWHM to account for the band-structure broadened d valence states into which the $2p_{3/2}$ core electrons are excited.

For a sample of finite thickness d and atomic number density ρ_a, the transmitted intensity decays exponentially with the number of atoms in the beam $N_a/A = \rho_a d$ according to Eq. (1). Since absorption and resonant scattering are related through Eq. (2), the Beer-Lambert absorption law can also be derived by considering resonant elastic forward scattering. To do so, one considers scattering by a thin atomic sheet so that the first Born approximation is valid. For a sheet thickness $\Delta \ll \lambda$, the spontaneously forward scattered fields are coherent, and the transmitted field is given by

$$E^q_{\text{trans}} = E^q_0 e^{ik\Delta}\{1 - i\lambda[r_0 Z + f'^q - if''^q]\rho_a\Delta\}. \qquad (3)$$

Neglecting the nonresonant (Thomson) term $r_0 Z$, the spontaneous intensity transmitted through the sample with N_a atoms in the beam of cross sectional area A is

$$I^q_{\text{trans}} = I^q_0\left\{1 - 2\lambda\frac{N_a}{A}f''^q + \lambda^2\frac{N^2_a}{A^2}[(f'^q)^2 + (f''^q)^2]\right\}. \qquad (4)$$

TABLE I. Polarization dependent parameters for the L_3 resonances of Fe, Co, and Ni metals. Listed are the atomic number densities ρ_a, the resonance energies and wavelengths, and the polarization dependent ($q = 0, \pm$) peak experimental cross sections σ^q_0 (1 Mb $= 10^{-4}$ nm^2), assuming propagation along the magnetization direction. Γ^q_x is the polarization dependent dipole transition width which includes the number of valence holes N_h, and Γ is the natural decay energy width [15].

	ρ_a [atoms/nm^3]	$\mathcal{E}_0$ [eV]	λ_0 [nm]	σ^+_0 [Mb]	σ^0_0 [Mb]	σ^-_0 [Mb]	Γ^+_x [meV]	Γ^0_x [meV]	Γ^-_x [meV]	Γ [eV]
Fe	84.9	707	1.75	8.8	6.9	5.0	1.37	1.08	0.78	0.36
Co	90.9	778	1.59	7.9	6.25	4.65	1.208	0.96	0.715	0.43
Ni	91.4	853	1.45	5.1	4.4	3.7	0.675	0.575	0.48	0.48

The first term is the incident intensity, and the second term is the absorption loss (minus sign) in linear response. Within the Born approximation, the absorption loss arises from the destructive interference of the incident field with the coherently forward scattered field. The third term is the forward scattered gain (plus sign) due to the coherent superposition of the fields scattered by the atoms in the sheet which scales as N_a^2. It is larger than the incoherently scattered intensity $I_0^q 4\pi N_a[(f'^q)^2 + (f''^q)^2]/A$, neglected in Eq. (4), by the coherent enhancement factor

$$\mathcal{G}_{\text{coh}} = \frac{N_a \lambda^2}{4\pi A}. \tag{5}$$

Here, $d\Omega_{\text{coh}} = \lambda^2/A$ is the solid angle of coherent forward scattering. The total field transmitted through a sample of arbitrary thickness $d = N\Delta$ is obtained by using the Darwin-Prins dynamical scattering summation of Eq. (3) over N thin sheets, which yields the exponential Beer-Lambert law, Eq. (1) [16]. Remarkably, for forward scattering, the longitudinal coherence length $\ell_c \simeq \lambda^2/\Delta\lambda$ does not enter [17] since the phases of the forward scattered fields are always referenced to those of the incident fields. Thus, $\mathcal{G}_{\text{coh}}$ does not depend on the atomic positions along the thickness d of the sample, and it is the same for a solid and a gas of the same area density N_a/A.

As the incident intensity is increased, the Kramers-Heisenberg-Dirac perturbation theory leads to unphysical results since it does not account for population changes in the excited state. This is overcome by the density matrix formalism which yields the time-dependent ground, $\rho_{11}(t)$, and excited state, $\rho_{22}(t) = 1 - \rho_{11}(t)$, populations as solutions of the optical Bloch equations [14].

In the presence of stimulation, we can write the atomic scattering length as the sum of a spontaneous (subscript "0") and stimulated nonlinear (subscript "NL") part according to

$$f'^q = r_0 Z + f'^q_0 + f'^q_{\text{NL}}, f''^q = f''^q_0 + f''^q_{\text{NL}}, \tag{6}$$

and the usual Beer-Lambert law, Eq. (1), is replaced by

$$I^q_{\text{trans}} = I_0^q e^{-2\lambda(f''^q_0 + 2f''^q_{\text{NL}})\rho_a d}. \tag{7}$$

The spontaneous absorption cross section $\sigma_{\text{abs}} = 2\lambda f''^q$ with $f''^q = f''^q_0$ in Eq. (1) becomes,

$$\sigma_{\text{abs}} = 2\lambda[f''^q_0 + 2f''^q_{\text{NL}}]. \tag{8}$$

Here, f''^q_0 is given by the spontaneous expression Eq. (2), and the nonlinear scattering length f''^q_{NL} is dependent on the excited state population per atom $\rho_{22}^q(t)$ obtained from the Bloch equations, integrated over the duration τ_c of the incident transform limited pulse, times a superradiantlike enhancement factor. If τ_c is much longer than the Auger decay time ($\hbar/\Gamma = 1.5$ fs for Co $2p_{3/2}$), $\rho_{22}^q(t)$ reaches an

equilibrium value $\rho_{22}^q(\infty)$ (see Fig. 2) and the nonlinear scattering length is given by the analytical expression

$$f''^q_{\text{NL}} = -f''^q_0 \underbrace{\frac{I_0^q \Gamma_x^q \mathcal{G}_{\text{coh}} \lambda^3/(8\pi^2 c)}{(\hbar\omega - \mathcal{E}_0)^2 + (\Gamma/2)^2 + I_0^q \Gamma_x^q \mathcal{G}_{\text{coh}} \lambda^3/(4\pi^2 c)}}_{\tilde{\rho}_{22}^q(\infty)}. \tag{9}$$

Here, $\tilde{\rho}_{22}^q(\infty)$ is an effective excited state population that, at resonance, $\hbar\omega = \mathcal{E}_0$, is given by the true excited state population $\rho_{22}^q(\infty)$ times a superradiantlike enhancement factor

$$\tilde{\rho}_{22}^q(\infty) = \rho_{22}^q(\infty)\left(1 + \frac{\mathcal{G}_{\text{coh}}}{1 + I_0^q \Gamma_x^q \mathcal{G}_{\text{coh}} \lambda^3/(\pi^2 c \Gamma^2)}\right), \tag{10}$$

that arises from the coherent (collective) response of all N_a atoms in the beam and lowers the stimulation threshold by a factor $\mathcal{G}_{\text{coh}}$. The nonlinear contribution f''^q_{NL} is seen to have the opposite sign of the spontaneous contribution f''^q_0. In the limit of high incident intensity, we simply have $\tilde{\rho}_{22}^q(\infty) = 0.5$ and $2f''^q_{\text{NL}} = -f''^q_0$ and, according to Eq. (7), the sample becomes transparent.

In Fig. 2, we show the increase of $\tilde{\rho}_{22}^q(\tau_c)$ for L_3 resonant excitation of a 20 nm thick Co metal film with incident intensity and different coherent pulse lengths τ_c, calculated by numerical solution of the optical Bloch equations with the parameters in Table I [blue curves in Fig. 1(a)]. We accounted for the bandwidth dependence on pulse length (coherence time) by the Gaussian relation, $\tau_c \Delta\mathcal{E} = 1.825$ eV fs, and treated the resonance broadening due to band structure effects by Gaussian convolution with FWHM 1.4 eV, as for the spontaneous case shown in Fig. 1(b). With increasing coherence time τ_c relative to the core hole life time, the threshold is shifted to lower intensity and the Rabi oscillations are suppressed. Figure 2(b) shows $\tilde{\rho}_{22}^q(\tau_c)$ plotted versus the total intensity per coherent pulse
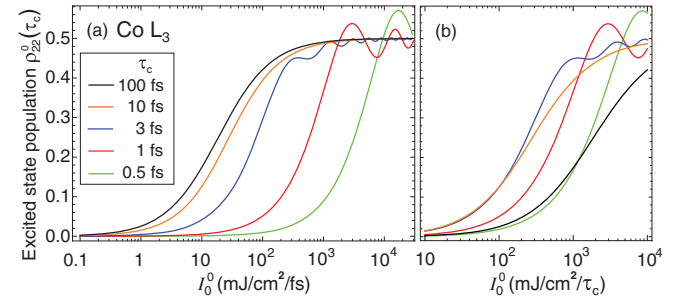

FIG. 2 (color). (a) $\tilde{\rho}_{22}^q(\tau_c)$ as a function of linearly polarized incident intensity I_0^0 for different coherence times τ_c of the incident pulses for the L_3 edge of a 20 nm thick Co metal film. We assumed resonance excitation, $\hbar\omega = \mathcal{E}_0$, and experimental peak cross sections as discussed in the text. (b) Same as in (a) as a function of the incident fluence per coherence time of the pulse.

of length τ_c, in units of $[\text{mJ/cm}^2/\tau_c]$. The stimulated threshold is seen to be lowest for coherent pulses in the 3–10 fs range.

Figure 3(a) shows the effective polarization dependent absorption cross section for Co given by Eq. (8) for three values of the incident intensity with f''^q_{NL} calculated according to Eq. (9). In Fig. 3(b), we illustrate the thickness dependence of the absorption contrast (linear polarization) obtained from Eq. (7) for several values of the incident intensity. At low intensity, the sample transmission decreases with increasing sample thickness d due to absorption. However, with increasing intensity, the transmitted intensity at large d is seen to decrease considerably
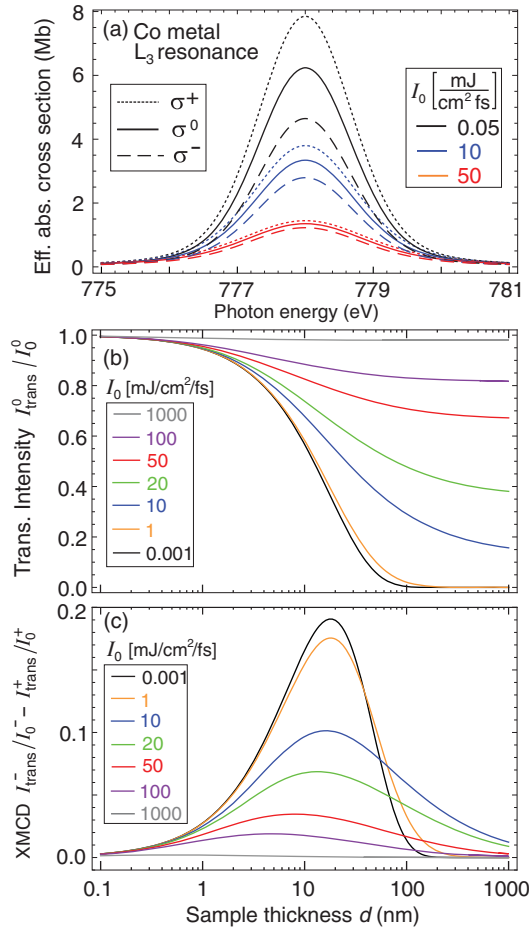

FIG. 3 (color). (a) Change of the effective polarization dependent absorption cross section $2\lambda(f''^q_0 + 2f''^q_{\text{NL}})$ for the L_3 resonance in Co metal for three incident intensity values, assuming alignment of the x-ray propagation direction with the film magnetization and the long coherence time limit, Eq. (9). The low intensity cross sections shown as black curves are nearly identical to the spontaneous ones shown in red in Fig. 1. (b) Dependence of the transmission contrast as a function of sample thickness and incident intensity for resonant L_3 excitation of a Co metal film due to charge absorption with linearly polarized light, according to Eq. (7). (c) Same as (b) for the transmitted XMCD contrast.

slower due to stimulated forward scattering. The magnetic XMCD contrast, plotted in Fig. 3(c), first increases with thickness up to a maximum around $d = 1/(\sigma_{\text{abs}}\rho_a) = 17$ nm, corresponding to one x-ray absorption length, before it also decreases.

Figure 4 shows the dependence of the transmitted intensity for the stimulated relative to the spontaneous case as a function of the incident intensity, calculated for Co metal with $d = 20$ nm and assuming resonant excitation. Both the effective absorption cross section and the transmitted intensity reveal a strong dependence on the incident intensity, with the spin related XMCD contrast (red curve) vanishing faster than the charge related x-ray absorption spectroscopy (XAS) contrast (black curve).

The inset reveals a particularly interesting thickness dependence of the transmitted XMCD intensity. For a thick sample of 100 nm, the remaining small spontaneous XMCD contrast of about 1.5%, which, according to Fig. 3(c), is greatly diminished by absorption, can actually be increased by nearly a factor of 5 upon stimulation.

The stimulated onset in Fig. 4 is predicted to be at least 3 orders of magnitude lower than for the stimulated effects observed before [2] for nonresonant excitation with broad bandwidth SASE pulses of 0.5 fs average coherence time [18]. The proposed resonant excitation with narrow bandwidth pulses of coherence times ~10 fs maximizes the interaction cross section and leads to a superradiantlike enhancement given by the second term in Eq. (10), which, for L_3 excitation of a Co film, has a maximum value of $\mathcal{G}_{\text{coh}} \sim 360$.

The dependence of the nonlinear contribution on the incident intensity, given by Eq. (9), may also be expressed
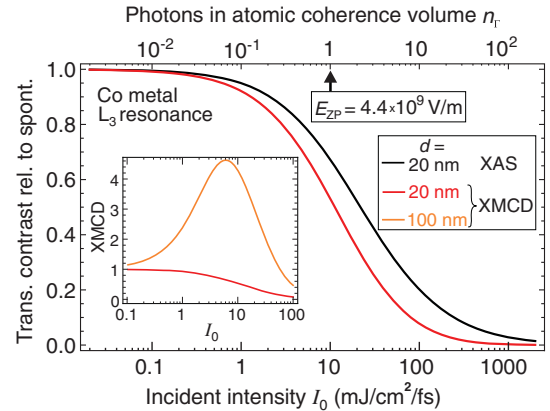

FIG. 4 (color). Dependence of the transmitted intensity according to Eq. (7) and Eq. (9) in the presence versus absence of stimulation for a 20 nm Co metal film as a function of incident intensity. The black curve represents the linear polarization or charge response $[I^0_{\text{trans}}]_{\text{stim}}/[I^0_{\text{trans}}]_{\text{spon}}$ and the red curve is the transmitted XMCD difference intensity $[I^-_{\text{trans}} - I^+_{\text{trans}}]_{\text{stim}}/[I^-_{\text{trans}} - I^+_{\text{trans}}]_{\text{spon}}$. The top scale is discussed in the text. The inset shows the relative transmitted XMCD contrast for film thicknesses of 20 nm (red) and 100 nm (orange) as a function of incident intensity.

in terms of the number of incident photons contained in a specific volume. If the volume is chosen to be the coherence volume V_{qk} per mode qk, then the associated number of photons n_{qk} is referred to as the photon degeneracy parameter. The incident photons that stimulate electronic decays, however, need to be present during the total atomic clock decay time $\hbar/\Gamma$ which defines the sample-specific atomic decay volume V_Γ. The two coherence volumes are given by

$$V_{qk} = \lambda^3 \frac{\hbar\omega}{\Delta(\hbar\omega)}, \qquad V_\Gamma = \lambda^3 \frac{\hbar\omega}{2\pi^2\Gamma}. \qquad (11)$$

The number of stimulating photons n_Γ in the volume V_Γ is that in the well-known stimulated correction term $1 + n_\Gamma$, and it can be expressed in terms of the incident polarization dependent intensity and field amplitude E_0^q as

$$n_\Gamma^q = \frac{1}{2\pi^2 c} \frac{\lambda^3}{\Gamma} I_0^q = \frac{\epsilon_0}{\pi^2} \frac{\lambda^3}{\Gamma} |E_0^q|^2 = \frac{|E_0^q|^2}{|E_{ZP}|^2}. \qquad (12)$$

On the right, we have introduced the zero-point (ZP) field E_{ZP} responsible for spontaneous radiative decays. For $n_\Gamma^q = 1$, the spontaneous and stimulated scattering intensities become the same, and the incident field E_0^q is equally effective in driving decays as the ZP field $|E_{ZP}|^2 = \pi^2\Gamma/(\epsilon_0\lambda^3)$, corresponding to one virtual photon in the volume V_Γ. This allows us to equate the intensity scale on the bottom of Fig. 4 with the number of photons n_Γ on top of the figure, and, for our case, the ZP field has the value $E_{ZP} \simeq 4.4 \times 10^9$ V/m.

---

*stohr@slac.stanford.edu
†andreas.scherz@xfel.eu

[1] P. Emma et al., Nat. Photonics **4**, 641 (2010); H. Tanaka et al., Nat. Photonics **6**, 540 (2012).

[2] N. Rohringer et al., Nature (London) **481**, 488 (2012); T. E. Glover et al., Nature (London) **488**, 603 (2012); M. Beye, S. Schreck, F. Sorgenfrei, C. Trabant, N. Pontius, C. Schüßler-Langeheine, W. Wurth, and A. Föhlisch, Nature (London) **501**, 191 (2013); C. Weninger, M. Purvis, D. Ryan, R. A. London, J. D. Bozek, C. Bostedt, A. Graf, G. Brown, J. J. Rocca, and N. Rohringer, Phys. Rev. Lett. **111**, 233902 (2013).

[3] L. Young et al., Nature (London) **466**, 56 (2010); J. P. Cryan et al., Phys. Rev. Lett. **105**, 083004 (2010); B. Nagler et al., Nat. Phys. **5**, 693 (2009); G. Doumy et al., Phys. Rev. Lett. **106**, 083002 (2011); L. Müller et al., Phys. Rev. Lett. **110**, 234801 (2013).

[4] D. Ratner et al., Phys. Rev. Lett. **114**, 054801 (2015).

[5] S. L. McCall and E. L. Hahn, Phys. Rev. Lett. **18**, 908 (1967); Phys. Rev. **183**, 457 (1969); For a review, see: L. Allen and J. H. Eberly, Optical Resonance and Two Level Atoms (Wiley, New York, 1975).

[6] S. Tanaka and S. Mukamel, Phys. Rev. Lett. **89**, 043001 (2002); J. D. Biggs, Yu Zhang, D. Healion, and S. Mukamel, Proc. Natl. Acad. Sci. U.S.A. **110**, 15597 (2013).

[7] B. D. Patterson, SLAC Report No. SLAC-TN-10-026 (2010).

[8] Amplified spontaneous inelastic emission has been observed by Rohringer et al. and Beye et al. (Ref. [2]) by use of intense broad bandwidth SASE pulses and nonresonant excitation. The required long gain length was achieved in the forward direction by use of a Ne gas of 10 absorption lengths thickness, or by a grazing emission geometry of a bulk Si sample.

[9] J. Stöhr, NEXAFS Spectroscopy, (Springer, New York, 1992).

[10] J. Stöhr and H. C. Siegmann, Magnetism: From Fundamentals to Nanoscale Dynamics, (Springer, New York, 2006).

[11] H. Ade and A. P. Hitchcock, Polymer **49**, 643 (2008).

[12] S. Eisebitt, J. Lüning, W. F. Schlotter, M. Lörgen, O. Hellwig, W. Eberhardt, and J. Stöhr, Nature (London) **432**, 885 (2004); T. Wang et al., Phys. Rev. Lett. **108**, 267403 (2012).

[13] L. J. P. Ament, M. van Veenendaal, T. P. Devereaux, J. P. Hill, and J. van den Brink, Rev. Mod. Phys. **83**, 705 (2011).

[14] R. Loudon, The Quantum Theory of Light, (Oxford, New York, 2000).

[15] M. O. Krause, J. Phys. Chem. Ref. Data **8**, 307 (1979); M. O. Krause and J. H. Oliver, J. Phys. Chem. Ref. Data **8**, 329 (1979).

[16] B. L. Henke, E. M. Gullikson, and J. C. Davis, At. Data Nucl. Data Tables **54**, 181 (1993).

[17] S. K. Sinha, Z. Jiang, and L. B. Lurio, Adv. Mater. **26**, 7764 (2014).

[18] I. A. Vartanyants et al., Phys. Rev. Lett. **107**, 144801 (2011).